

Amelioration of Symptomatic Alzheimer's Disease after Selective Impairment of p75^{NTR} Function in Adult Forebrain Excitatory Neurons

Xuetong Li,¹ Meng Xie,^{2,3,4} and Carlos F. Ibáñez^{1,2,5,6,7}

¹School of Life Sciences, Peking University, Beijing 100871, China, ²PKU-IDG/McGovern Institute for Brain Research, Peking-Tsinghua Center for Life Sciences, Peking University, Beijing 100871, China, ³School of Psychological and Cognitive Sciences, Peking University, Beijing 100871, China, ⁴Department of Medicine Huddinge, Karolinska Institute, Huddinge 14157, Sweden, ⁵Chinese Institute for Brain Research, Zhongguancun Life Science Park, Beijing 102206, China, ⁶Department of Neuroscience, Karolinska Institute, Stockholm 17177, Sweden, and ⁷Stellenbosch Institute for Advanced Study, Wallenberg Research Centre at Stellenbosch University, Stellenbosch 7600, South Africa

The p75 neurotrophin receptor (p75^{NTR}) contributes to the development of Alzheimer's disease (AD) pathology by enhancing amyloid precursor protein (APP) cleavage and amyloid plaque formation. However, the cell type-specific and temporal roles of p75^{NTR} in AD progression remain unclear. Here, we report that conditional knock-in of functionally impaired p75^{NTR} variants lacking the death domain (ADD) or transmembrane Cys²⁵⁹ (C259A) specifically in forebrain excitatory neurons of male and female 5xFAD mice significantly attenuated multiple AD-associated pathologies, including amyloid plaque accumulation, gliosis, neurite dystrophy, as well as learning and memory deficits. Hippocampal amyloid plaque burden was reduced to levels comparable with those found in whole-body knock-in mice. Strikingly, delaying introduction of p75^{NTR} variants until advanced disease stages produced comparable beneficial effects and rescued behavior performance in cognitively impaired animals. These findings suggest that blunting p75^{NTR} function can have beneficial effects even during symptomatic stages of AD, offering a potential therapeutic approach complementary to passive vaccination.

Key words: A-beta; amyloid; neurodegeneration

Significance Statement

Inactivation of p75^{NTR} has been reported to show various degrees of neuroprotection in Aβ-based mouse models of AD. As p75^{NTR} is expressed in several different cell types in the brain, it has been unclear whether the beneficial effects afforded arose from all cell types or only one. For therapeutic approaches to be viable in AD patients, any form of interference with its activity needs to demonstrate beneficial effects during symptomatic stages of the disease. Here, we show that replacement of native p75^{NTR} with signaling-impaired variants in forebrain excitatory neurons is sufficient to significantly alleviate neuropathological and behavioral outcomes in 5xFAD mice. Moreover, significant amelioration of neuropathology and cognitive deficits were achieved after acute disruption of p75^{NTR} during symptomatic AD stages.

Introduction

Alzheimer's disease (AD) is the most prevalent form of dementia. The generation and accumulation of neurotoxic fragments of amyloid beta (Aβ), generated from amyloid precursor protein (APP) through sequential proteolytic cleavage, is one primary cause of AD pathogenesis (also known as the amyloid hypothesis;

Beyreuther and Masters, 1991; Hardy and Allsop, 1991; Selkoe, 1991). Forebrain excitatory neurons express significant levels of APP which can be cleaved by the β-site secretase (BACE1) within its extracellular domain (Vassar et al., 1999). This cleavage generates a C-terminal fragment (CTFβ) which serves as a substrate for a γ-secretase to produce Aβ peptides of 40 or 42 amino acids,

Received Oct. 15, 2025; revised Dec. 22, 2025; accepted Jan. 8, 2026.

Author contributions: C.F.I. designed research; X.L. performed research; X.L. and M.X. analyzed data; C.F.I. wrote the paper.

We thank Lei Wang, Jocelyn Jia, Yankui Fu, and Shuo Zhang for technical and admin assistance. This work was supported by research grants to C.F.I. from Peking University, Chinese Institute for Brain Research, Beijing, and Swedish Research Council (Vetenskapsrådet, contract nr. 2024-03222) and a startup grant to M.X. from Swedish Research Council (Vetenskapsrådet, contract nr. 2021-01805).

The authors declare no competing financial interests.

Correspondence should be addressed to Carlos F. Ibáñez at carlos.ibanez@pku.edu.cn, carlos.ibanez@cibr.ac.cn.

This paper contains supplemental material available at: <https://doi.org/10.1523/JNEUROSCI.1939-25.2026>

<https://doi.org/10.1523/JNEUROSCI.1939-25.2026>

Copyright © 2026 the authors

the main component of the AD amyloid plaques (Selkoe, 2000; Bitan et al., 2003; Vassar et al., 2009). APP can also be cleaved by extracellular α -secretases (e.g., ADAM10) within the A β sequence to generate soluble APP α (sAPP α), thereby precluding cleavage by BACE1 and A β production. β -site and α -site secretases represent antagonistic processing alternatives of amyloidogenic and nonamyloidogenic cleavage of APP, respectively (Furukawa et al., 1996; Meziane et al., 1998; Stein et al., 2004).

p75 neurotrophin receptor (p75^{NTR}) is a member of the death receptor superfamily characterized by the presence of a 6 α -helix bundle known as the “death domain” (DD) in its intracellular region (Liepinsh et al., 1997). The intracellular domain of p75^{NTR} lacks catalytic activity and participates in signal transduction through ligand-induced recruitment and release of effector proteins (Dechant and Barde, 2002; Roux and Barker, 2002; Chao, 2003; Bronfman and Fainzilber, 2004; Underwood and Coulson, 2008; Ibáñez and Simi, 2012). At the cell surface, p75^{NTR} forms dimers stabilized by a disulfide-link formed by a highly conserved cysteine residue (Cys²⁵⁹) in its transmembrane domain that is essential for activation by neurotrophin ligands (Vilar et al., 2009). Expression of p75^{NTR} is upregulated upon brain injury and neuronal damage, and many studies have linked p75^{NTR} to neurodegenerative diseases (Ibáñez and Simi, 2012). Analyses of brains of AD patients and various animal models demonstrate increased p75^{NTR} expression during disease progression (Mufson and Kordower, 1992; Hu et al., 2002; Chakravarthy et al., 2012). Notably, our laboratory has previously shown that two signaling-deficient p75^{NTR} variants, Δ DD (lacking the DD) and C259A (with Ala replacing the highly conserved transmembrane Cys²⁵⁹ in the transmembrane domain), resulted in greater neuroprotective effects than the full knock-out of the receptor when introduced in the germline of 5xFAD mice (Yi et al., 2021). Mechanistically, this was achieved by the ability of these variants to slow down APP internalization and thereby interfere with the amyloidogenic pathway of APP processing (Yi et al., 2021). However, it remained unclear which p75^{NTR}-expressing cells were responsible for the neuroprotective effects, nor whether any neuroprotection could be achieved if the variants were to be expressed symptomatic disease stages.

In this study, we conditionally introduced the Δ DD and C259A variants of p75^{NTR} specifically into forebrain excitatory neurons of 5xFAD mice. This approach allowed to assess what level of neuroprotection could be achieved through the expression of these variants in a very restricted subset of neurons and whether any neuroprotection could be obtained by substantially delaying the introduction of p75^{NTR} variants to advanced, overtly symptomatic stages of the disease.

Materials and Methods

Mice. Animal care and experimental procedures were approved by the Laboratory Animal Welfare and Ethics Committee of Chinese Institute for Brain Research (CIBR-IACUC-028). Mice were housed in a 12 h light/dark cycle and fed a standard chow diet. The mouse lines utilized in this study are as follows: 5xFAD (Oakley et al., 2006); Camk2a-Cre, JAX Laboratory (#005359); Camk2a-CreERT2, JAX Laboratory, (#012362); conditional knock-in p75^{NTR} Δ DD^{fl} and C259A^{fl} generated for this study by Cyagen; constitutive knock-in p75^{C259A} (Tanaka et al., 2016). All mice were male of C57BL/6J background.

Genomic DNA extraction and PCR. The Biotime Genomic DNA Extraction Kit was used to extract genomic DNA from frozen tissue of mice of different genotypes. Electrophoretic results showed bands at 760 bp corresponding to the recombined flox allele and bands at

2,000 bp corresponding to the unrecombined flox allele. Primers sequences for PCR are as follows:

C259A-flox-F: 5'-GCCTCTGATCAGCTCTAAAAGTGCC-3'
 C259A-flox-R: 5'-ATCCTCAGTGTGCCCTCTTAC-3'
 Δ DD-flox-F: 5'-GGACACTTGCTGCAGTTATAAC-3'
 Δ DD-flox-R: 5'-ACAGAGGCCCTACACAGAGAT-3'

Antibodies. The primary antibodies used for immunofluorescence (IF) and immunoblotting (WB) are described in Table 1.

Western blotting. Frozen tissue was collected and thawed on ice, the tissue was minced, and an appropriate amount of RIPA Buffer was added, and the tissue was lysed on ice for 30 min. The lysed samples were centrifuged at 12,000 \times g for 10 min at 4°C, and the supernatant was taken. The protein concentration contained in the samples was determined using a BCA kit (Solarbio). The samples were separated by electrophoresis using 10% SDS-PAGE, and the protein samples were transferred to PVDF membranes using the Bio-Rad semidry transfer system, blocked with 5% skimmed milk for 1 h, and the primary antibody was incubated at 4°C overnight. On the second day, the membrane was washed three times with TBST for 10 min each time, and then the HRP-conjugated secondary antibody was incubated at room temperature for 1 h. The membrane was washed three times with TBST and then blotted. The analysis and statistics of the results were performed using ImageJ software (NIH), and the histograms of the statistical results were produced using GraphPad.

Immunohistochemistry. For immunohistochemistry, cryostat sections (14 μ m) of mouse brain prepared as previously described were washed in PBS and preincubated in PBS containing 5% donkey serum and 0.2% Triton X-100 for 30 min. Sections were then processed for immunostaining by overnight incubation at 4°C with primary antibodies including 6E10 (1:1,000), GFAP (1:500), Iba1 (1:500), vimentin (1:500), RTN3 (1:500), washed in PBS, and incubated in fluorophore-conjugated secondary antibodies (Invitrogen) diluted 1:1,000 in PBS. Sections were washed, mounted in Fluoromount, and examined with a Zeiss LSM900 confocal microscope.

Protein fractionation and A β ELISA. For extraction of A β fragments, we followed a fractionation protocol previously described. Dissected frozen mouse hippocampal tissue (9-month-old) was thawed on ice and homogenized using a manual Dounce homogenizer, in Tris-buffered saline (25 mM Tris, 140 mM NaCl, pH 7.2–7.6) containing protease and phosphatase inhibitor (MCE). Homogenates were then ultracentrifuged at 100,000 \times g for 1 h at 4°C. The supernatant, which constitutes the soluble materials, was collected as the Tris-buffered saline fraction. The pellet of the Tris-buffered saline fraction was resuspended in RIPA buffer (Sigma-Aldrich) containing protease and phosphatase inhibitors by trituration 15 times with a 1 ml pipette. Samples were incubated at 4°C for 1 h with agitation and ultracentrifuged at 100,000 \times g for another hour at 4°C and were collected as RIPA fraction. The Tris-buffered saline and RIPA fractions were stored at -80°C until further analysis. The content of A β 1–42 in the Tris-buffered saline and RIPA fractions was assessed using the Human A β 1–42 enzyme-linked immunosorbent assay (ELISA) Kit (R&D) according to the

Table 1. Primary antibodies used for immunofluorescence (IF) and immunoblotting (WB)

Antibody (catalog nr.)	Supplier	IF dilution	WB dilution
A β (1–16), 6E10 (803002)	BioLegend	1:1,000	
GAPDH (G9545)	Sigma-Aldrich		1:10,000
GFAP (AB7260)	Abcam	1:500	
Iba1 (019-19741)	Wako	1:500	
NeuN (ab104224)	Abcam	1:500	
p75NTR (DD, ab52987)	Abcam	1:100	1:400
p75NTR (ECD, AF1157)	R&D	1:200	1:200
RTN3 (ABN1723)	Merck/Millipore	1:500	
Vimentin (PA1-10003)	Thermo Invitrogen	1:500	

manufacturer's instructions. The concentration of A β 1–42 was determined by the absorbance value detected using a microplate reader (BioTek Cytation 5) at 450 and 590 nm and then normalized to total protein concentration.

Image analysis. For each mouse, at least five brain coronal sections were quantified. In each brain section, mosaic images in hippocampus were captured. ImageJ software was used to quantify positive signal area for the different markers. For A β , GFAP, Iba1, and vimentin, percentage of positive signal area was normalized to total area of hippocampus. For RTN3, positive signal area within A β plaques was for quantification and expressed as percentage of total A β plaque area.

Novel object recognition. The novel object recognition (NOR) test for mice consists of exposure training, followed by a short-term memory (STM) test 3 h after training, a long-term memory (LTM) test 24 h later. The objects are chosen based on similarities in dimensions and complexity. Tests are carried out in an acrylic box (20.32 × 40.5 × 16 cm L × W × H) that is sanitized, together with the objects, with 75% ethanol between each experiment. The time spent with an object includes direct visual orientation toward an object within half the body length of the object, sniffing, touching, or climbing on the object. The tests are video-recorded, and preference scores are calculated as time spent with the novel object minus time spent with the familiar object divided by the total time spent with both objects. Positive scores indicate preferences for the novel object; negative scores show preferences for the familiar object.

Barnes maze. Twenty 5-cm-diameter holes were evenly distributed around the edge of a 90-cm-diameter circular platform. Three spatial cues of different shapes and colors were placed around the disk and kept constant during the experiment, and the platform was ~1 m above the ground with a strong light above it. Before the first training session, the mice were placed in an escape box for 1 min, and then the mice were placed in the center of the platform with a black box, which was removed after 10 s and recording began. During each training session, mice were free to explore the maze until they entered the escape box or for a period of 3 min. For each mouse, the escape box was always located below the same hole. Prior to each day's experiment, the platform would be rotated 90° to avoid the influence of olfactory cues on the experiment. Mice were trained once a day for 5 d. A memory test was performed 3 h after the last training session. During the memory test phase, the escape box was removed and the mice explored freely in the maze for 90 s. The memory level of the mice was quantitatively assessed by calculating the exploration time spent in the target quadrant.

Statistical analysis. Statistical Analysis Software (SAS Institute) and GraphPad Prism (versions 4 or 8; GraphPad Software) were used for statistical analyses. Experimental data was collected from multiple experiments and reported as the treatment mean ± SEM. Statistical significance was calculated using the statistical analysis indicated in the figure legends. *p* value of <0.05 was considered statistically significant. **p* < 0.05, ***p* < 0.01, ****p* < 0.001, *****p* < 0.0001 versus control groups.

Results

Generation of conditional knock-in mice expressing signaling-deficient p75^{NTR} variants in forebrain excitatory neurons

To investigate the effects of signaling-deficient p75^{NTR} variants in a cell type-specific and time-dependent manner, we generated conditional alleles of the mouse *Ngfr* gene encoding p75^{NTR} (herein termed $\Delta DD^{fl/fl}$ and $C259A^{fl/fl}$) that allow expression of mutant ΔDD and $C259A$ variants after Cre-mediated recombination (Fig. S1A,B). We confirmed that the engineered alleles expressed normal levels of p75^{NTR} prior to recombination (Fig. S2A,B). In order to specifically introduce ΔDD and $C259A$ p75^{NTR} variants into forebrain neurons, we employed the *Camk2a-Cre* driver which induces robust and specific recombination in forebrain excitatory neurons (Tsien et al., 1996). We verified the specificity of this driver

by breeding it to Ai14 reporter mice and assessed the proportion of tdTomato⁺ cells among the NeuN⁺ subpopulation. tdTomato expression began at 2 weeks of age, reaching 90% by 2 months in hippocampus and cortex (Fig. S3A,B), and was restricted to forebrain neurons, as no tdTomato signal was detected in the midbrain or cerebellum, and no overlap was observed between tdTomato and either GFAP or Iba1 in the cortex or hippocampus (Fig. S3C–E). We generated mice carrying the *Camk2a-Cre* driver and $\Delta DD^{fl/fl}$ and $C259A^{fl/fl}$ alleles (herein referred to as ΔDD^{Camk2a} and $C259A^{Camk2a}$, respectively). Cre-mediated recombination was verified by PCR from forebrain tissue of 2-month-old mice (Fig. S3F,G). At the protein level, deletion of the death domain in ΔDD^{Camk2a} mice was verified by Western blotting of hippocampus extracts using antibodies directed to either the extracellular (ECD) or death domains (DD; Fig. S4A,B). Similar results were obtained by immunohistochemistry in cortex and hippocampus of 2-month-old ΔDD^{Camk2a} mice (Fig. S4C). Importantly, recombination specificity was confirmed by analysis of sections through the basal forebrain of these mice where the *Camk2a-Cre* driver is inactive. In this case, the DD signal was lost in cortex and hippocampal neurons but still preserved in basal forebrain neurons (Fig. S4C). Together, these results confirm the successful generation of conditional knock-in mice that specifically express signaling-deficient p75^{NTR} variants in forebrain neurons.

Signaling-deficient p75^{NTR} variants in forebrain excitatory neurons of 5xFAD mice reduce A β plaque burden and enhance nonamyloidogenic APP processing

We generated 5xFAD mice expressing signaling-deficient p75^{NTR} variants in forebrain excitatory neurons (termed $\Delta DD^{Camk2a}/5xFAD$ and $C259A^{Camk2a}/5xFAD$, respectively) and assessed their amyloid plaque burden in hippocampus and cortex at 6.5 and 9 months by A β immunohistochemistry in comparison with control 5xFAD mice carrying nonrecombined p75^{NTR} alleles ($\Delta DD^{fl/fl}/5xFAD$ and $C259A^{fl/fl}/5xFAD$, respectively). Both $\Delta DD^{Camk2a}/5xFAD$ and $C259A^{Camk2a}/5xFAD$ mice showed a significant reduction in A β plaque burden to ~50% of control 5xFAD levels in hippocampus and cortex at both ages and in both male (Fig. 1A–C) and female (Fig. S5A–C) mice. Importantly, A β plaque burden in thalamus remained unchanged (Fig. 1D), in agreement with the specificity of the *Camk2a-Cre* driver. We also noted that the proportion of large A β plaques (>50 μ m diameter) decreased, while that of small plaques (<30 μ m diameter) increased in the brains of $\Delta DD^{Camk2a}/5xFAD$ and $C259A^{Camk2a}/5xFAD$ mice (Fig. 1E), indicating that A β plaque burden was reduced in both number and size by the conditional mutations. Interestingly, A β plaque levels in $C259A^{Camk2a}/5xFAD$ mice was comparable with those observed in constitutive, whole-body p75^{C259A}/5xFAD mice (Fig. 1A,B), suggesting that restricted expression of this p75^{NTR} variant in only postnatal forebrain excitatory neurons can confer similar neuroprotection to that afforded by whole-body expression from birth (as that reported in our earlier study by Yi et al., 2021).

Next, we quantified A β 1–42 levels by ELISA after differential detergent extraction from hippocampus of 9-month-old mice and found that both $\Delta DD^{Camk2a}/5xFAD$ and $C259A^{Camk2a}/5xFAD$ mice exhibited lower levels of A β 1–42 monomers (assessed in the supernatant of the TBS fraction) and oligomers (supernatant of the RIPA fraction) compared with their respective control 5xFAD mice (Fig. 1F,G). Finally, we assessed the levels of APP fragments soluble APP alpha (sAPP α) and carboxy-terminal fragment beta (CTF β) in hippocampal lysates from 9-month-old mice and found increased sAPP α levels

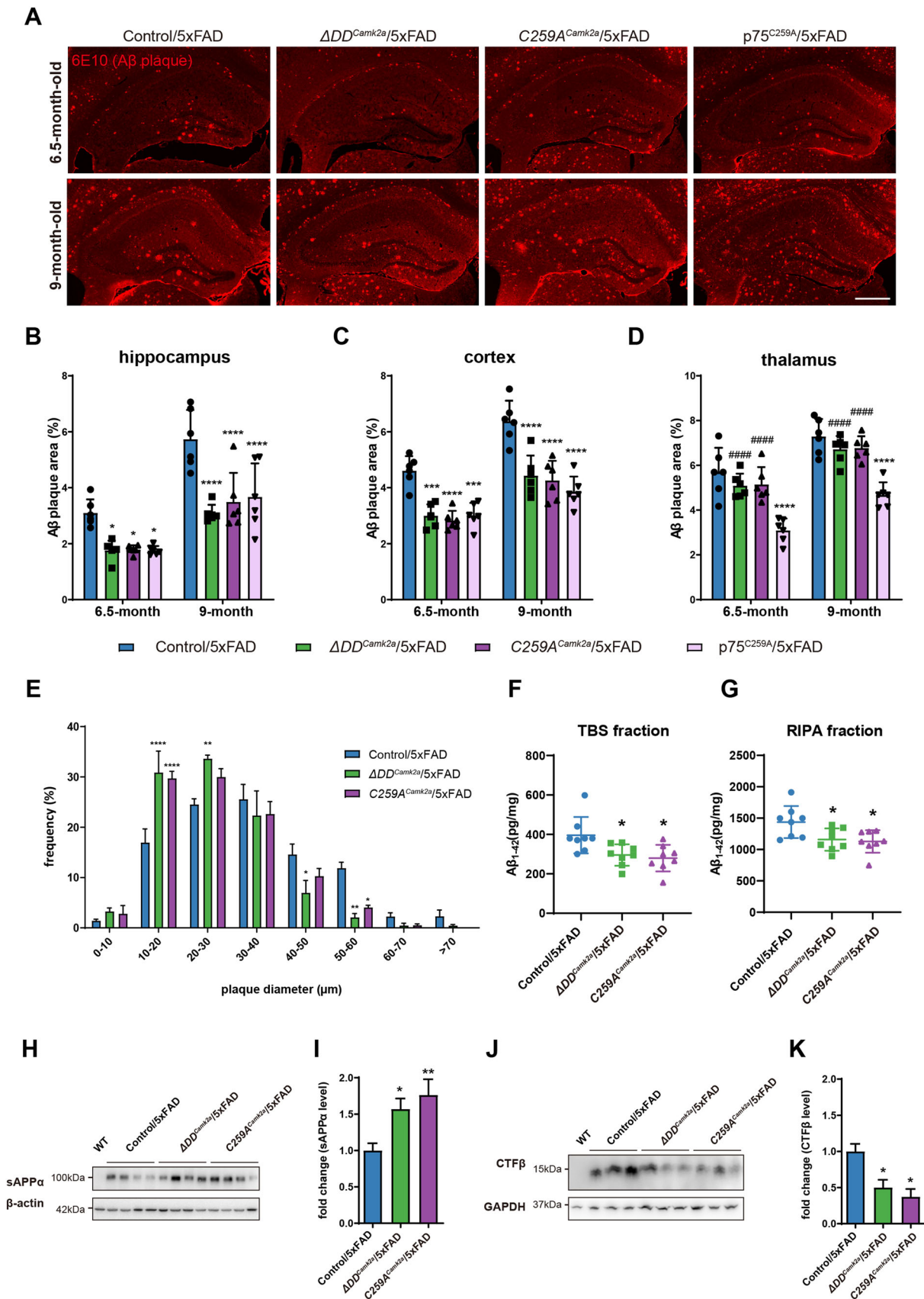


Figure 1. Signaling-deficient p75^{NTR} variants in forebrain excitatory neurons of 5xFAD mice reduce A β plaque burden and enhance nonamyloidogenic APP processing. **A**, Immunostaining of A β plaques with 6E10 antibody in the hippocampus of Control/5xFAD, $\Delta DD^{Camk2a}/5xFAD$, $C259A^{Camk2a}/5xFAD$, and $p75^{C259A}/5xFAD$ mice of the indicated ages. Scale bar, 500 μm . **B–D**, Quantification of A β plaque burden in the hippocampus (**B**), cortex (**C**), and thalamus (**D**) of Control/5xFAD, $\Delta DD^{Camk2a}/5xFAD$, $C259A^{Camk2a}/5xFAD$, and $p75^{C259A}/5xFAD$ mice as indicated. Histogram shows the percentage of hippocampal area occupied by A β plaques (mean \pm SD, $N = 6$ animals per group). All mice included in this analysis were male. Two-way ANOVA followed

(Fig. 1H,I) but decreased CTF β levels (Fig. 1J,K) in $\Delta DD^{Camk2a}/5xFAD$ and $C259A^{Camk2a}/5xFAD$ mice compared with 5xFAD controls, indicating a bias toward nonamyloidogenic APP processing in the mutant mice. Together, these results demonstrate that interfering with p75^{NTR} function only in forebrain excitatory neurons is sufficient to reduce A β plaque deposition to levels comparable with a systemic intervention.

Reduced brain AD histopathology in 5xFAD mice expressing signaling-deficient p75^{NTR} variants in forebrain neurons

Accumulation of A β plaques induces the activation of astrocytes and microglia which can lead to neuroinflammation and synaptic loss (Strooper and Karran, 2016; Singh, 2022; Deng et al., 2024). As expected, astrogliosis and microgliosis were significantly increased at 6 and 9 months of age in hippocampus of control 5xFAD mice ($\Delta DD^{fl/fl}/5xFAD$ and $C259A^{fl/fl}/5xFAD$), as shown by increased immunostaining for glial fibrillary acidic protein (GFAP) and ionized calcium-binding adaptor molecule 1 (Iba1) compared with non-AD mice (Fig. 2A,B). Activated astrocytes and microglia also showed morphological changes and clustered around A β plaques. In contrast, 5xFAD mice expressing signaling-deficient p75^{NTR} variants in forebrain neurons showed significantly reduced astrocyte and microglia activation (Fig. 2A–D). Vimentin-expressing astrocytes are a subset of pro-inflammatory, disease-associated cells that contribute to amplify A β toxicity promoting neurodegeneration (Habib et al., 2020; Lee and Quintana, 2024). Vimentin-expressing astrocytes were detected only in 5xFAD brains and were concentrated in the dentate gyrus area and along the hippocampal border (Fig. 2E). The hippocampus of $\Delta DD^{Camk2a}/5xFAD$ and $C259A^{Camk2a}/5xFAD$ mice showed ~50% reduction in vimentin expression compared with control 5xFAD mice (Fig. 2E,F), suggesting reduced neuroinflammation after disruption of p75^{NTR} signaling in forebrain neurons. Finally, we assessed the accumulation of reticulon 3 (RTN3), a protein that marks degenerating neurites (Hu et al., 2007), in cortex and hippocampus of 5xFAD mice expressing different p75^{NTR} alleles. At 9 months of age, control 5xFAD mice exhibited pronounced RTN3 immunostaining clustering around A β plaques in both cortex and hippocampus (Fig. 2G). In contrast, RTN3 immunoreactivity was significantly reduced in both $\Delta DD^{Camk2a}/5xFAD$ and $C259A^{Camk2a}/5xFAD$ mice (Fig. 2G,H). Together, these data indicate reduced gliosis and neurodegeneration in the forebrain of 5xFAD mice expressing signaling-deficient p75^{NTR} variants, in agreement with their decreased A β burden.

Improved learning and memory in 5xFAD mice expressing ΔDD and $C259A$ p75^{NTR} variants in forebrain neurons

5xFAD mice show significant learning and memory impairments at 6 months of age (Forner et al., 2021). We evaluated learning

and memory in 6-month-old 5xFAD male mice expressing different p75^{NTR} alleles using the Barnes maze, a widely used test of hippocampal-dependent spatial learning (Barnes, 1979; Bach et al., 1995), and the novel object recognition (NOR) test, which assesses the mouse's natural preference to explore a novel object over a familiar one. During the training phase of the Barnes maze, wild-type mice demonstrated normal learning ability, gradually reducing their latency to enter the escape tunnel to about 40 s (Fig. 3A). In contrast, control 5xFAD mice (both $\Delta DD^{fl/fl}/5xFAD$ and $C259A^{fl/fl}/5xFAD$) showed impaired learning, with essentially constant escape latencies throughout the training sessions (Fig. 3A). Importantly, learning ability was significantly rescued in both $\Delta DD^{Camk2a}/5xFAD$ and $C259A^{Camk2a}/5xFAD$ mice, with escape latencies reaching wild-type levels by the last training session (Fig. 3A). In the memory test conducted 3 h after the last training session, wild-type mice and 5xFAD mice expressing mutant p75^{NTR} variants spent most of their exploration time in the target quadrant containing the escape tunnel, while control 5xFAD mice spent only ~25%, consistent with chance probability (Fig. 3B), suggesting improved spatial memory in $\Delta DD^{fl/fl}/5xFAD$ and $C259A^{fl/fl}/5xFAD$ mice. In the training session of the NOR test, no preference for any of the two (identical) objects was observed in any line of mice, as expected (Fig. 3C). In probe tests performed 3 and 24 h after the training, wild-type mice spent ~40% more time exploring the new object (Fig. 3D,E). Control 5xFAD mice showed no preference, while both $\Delta DD^{fl/fl}/5xFAD$ and $C259A^{fl/fl}/5xFAD$ mice demonstrated a trend toward recognizing the novel object more frequently, although statistical significance was not reached for these groups (Fig. 3D,E).

Significant amelioration of AD neuropathology and cognitive function after acute disruption of p75^{NTR} activity during symptomatic AD stages

The observation that impaired p75^{NTR} function in forebrain excitatory neurons provided significant neuroprotection in 5xFAD mice prompted us to investigate whether beneficial effects could still be observed if the mutations were to be introduced after the onset of AD symptoms in these mice. To this end, we used the *Camk2a-CreERT2* driver, which can induce recombination in forebrain neurons after administration of tamoxifen (Madisen et al., 2010). We first verified neuron-specific recombination by immunostaining for NeuN, GFAP, and Iba1 after tamoxifen administration in 2-, 4-, and 6-month-old *Camk2a-CreERT2;Ai14* reporter mice (Fig. S6A–C). Recombination rates were comparable across different injection ages, reaching 70–80% in the hippocampus and 50–70% in the cortex (Fig. S6D,E). In line with a previous report (Erdmann et al., 2007), ~20% recombination was observed in neurons of mice injected with vehicle (Fig. S6D–F).

by Tukey's multiple-comparisons test. * $p < 0.05$, ** $p < 0.01$, *** $p < 0.001$, **** $p < 0.0001$ versus Control/5xFAD. #### $p < 0.0001$ versus p75^{C259A}/5xFAD. **E**, Frequency distribution analysis for the plaque diameter in the hippocampus of 6.5-month-old Control/5xFAD, $\Delta DD^{Camk2a}/5xFAD$, and $C259A^{Camk2a}/5xFAD$ mice (mean \pm SEM, $N = 3$ animals per group). For each animal, more than 300 plaques in the hippocampus are quantified. Two-way ANOVA followed by Tukey's multiple-comparisons test. **F**, **G**, Quantitative ELISA determinations of A β 1–42 in hippocampus of 9-month-old Control/5xFAD, $\Delta DD^{Camk2a}/5xFAD$, and $C259A^{Camk2a}/5xFAD$ mice. TBS fraction (**F**) refers to the soluble fraction after Tris-buffered saline extraction and contains A β monomers. RIPA fraction (**G**) refers to the soluble fraction after RIPA buffer extraction from the Tris-buffered Saline pellet and contains oligomeric A β . Shown is mean \pm SEM, $N = 8$ animals per group. One-way ANOVA followed by Tukey's multiple-comparisons test. All mice included in this analysis were male. **H**, Western blot analysis of soluble APP alpha (sAPP α) in the Tris-buffered saline fraction of hippocampal extraction from 9-month-old 5xFAD mice carrying conditional knock-in p75^{NTR} variants. sAPP α was detected by 6E10 antibody. The bottom panel shows β -actin as a control for equal loading amount. **I**, Quantification of sAPP α (mean \pm SD) normalized to internal control and expressed relative to levels in Control/5xFAD. $N = 8$ animals per group. **J**, Western blot analysis of CTF beta (CTF β) in the RIPA fraction of hippocampal extraction from 9-month-old 5xFAD mice carrying conditional knock-in p75^{NTR} variants. CTF β was detected by 6E10 antibody. The bottom panel shows GAPDH as a control for equal loading amount. **K**, Quantification of CTF β (mean \pm SD) normalized to internal control and expressed relative to levels in Control/5xFAD. $N = 3$ animals per group.

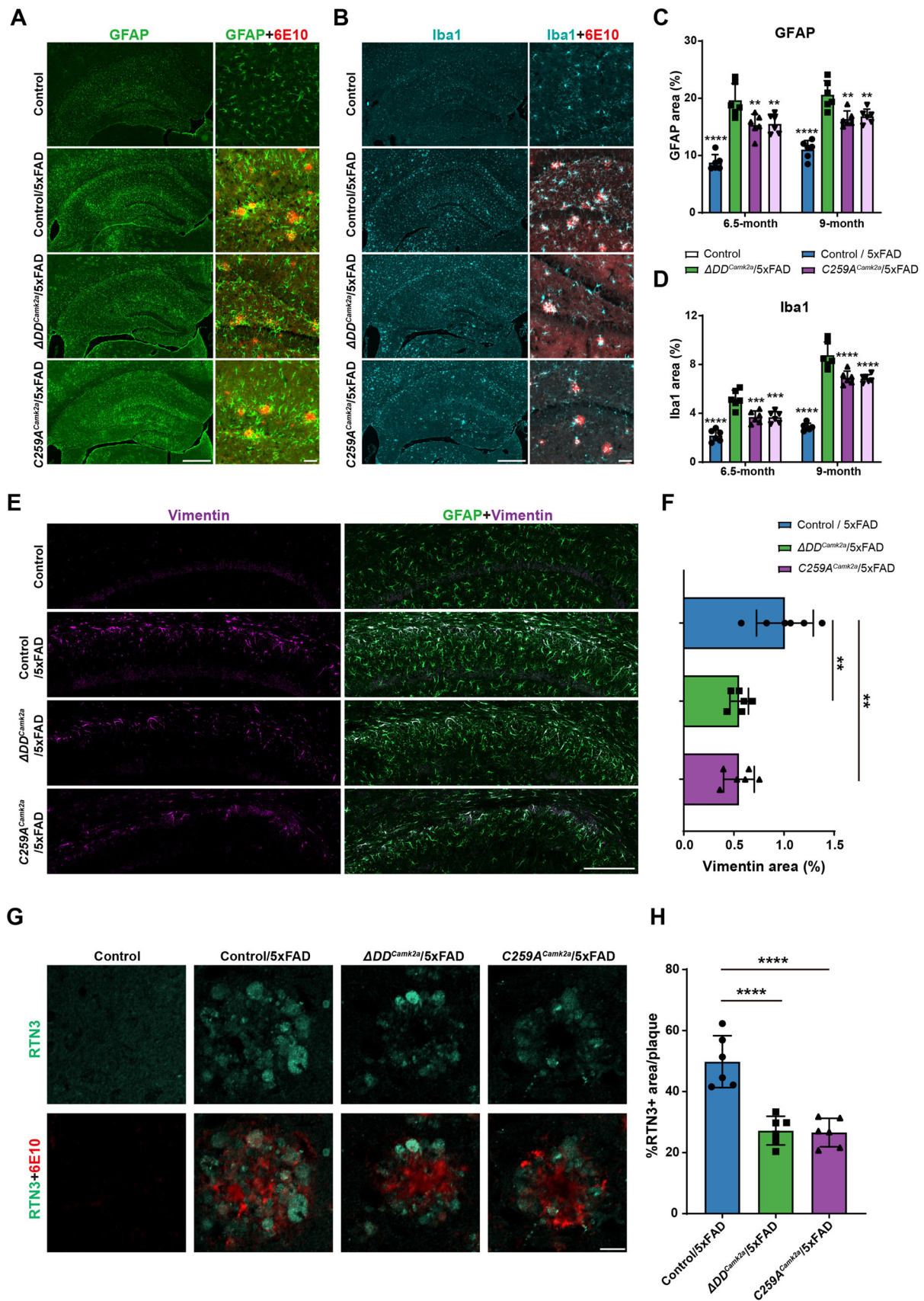


Figure 2. Reduced brain AD histopathology in 5xFAD mice expressing signaling-deficient p75^{NTR} variants in forebrain neurons. **A**, Immunostaining of glial fibrillary acidic protein (GFAP) in the hippocampus of 6.5-month-old Control, Control/5xFAD, $\Delta DD^{Camk2a}/5xFAD$, and $C259A^{Camk2a}/5xFAD$ mice. Scale bar, 500 μ m. Right panels show coimmunostaining of GFAP and A β plaques at a higher magnification. Scale bar, 50 μ m. **B**, Immunostaining of ionized calcium-binding adaptor molecule 1 (Iba1) in the hippocampus of 6.5-month-old Control, Control/5xFAD, $\Delta DD^{Camk2a}/5xFAD$, and $C259A^{Camk2a}/5xFAD$ mice. Scale bar, 500 μ m. Right panels show coimmunostaining of Iba1 and A β plaques at a higher magnification. Scale bar, 50 μ m. **C**, Quantification of

We introduced the *Camk2a-CreERT2* driver in $\Delta DD^{fl/fl}/5x\text{FAD}$ and $C259A^{fl/fl}/5x\text{FAD}$ mice and assessed AD neuropathology in their progeny, herein referred to as $\Delta DD^{CreERT2}/5x\text{FAD}$ and $C259A^{CreERT2}/5x\text{FAD}$ mice, respectively. Tamoxifen was administered at 2, 4, or 6 months, and analyses were conducted at 9 months of age (Fig. 4A), with the 2 months time point being comparable with the noninducible *Camk2a-Cre* driver, which achieves maximal Cre recombination at this age (see above). To our surprise, we found comparable reduction in A β plaque levels in both hippocampus and cortex at all injection ages (Fig. 4B–F), suggesting that acute disruption of p75^{NTR} activity at advanced AD stages can still afford significant neuroprotective effects. In agreement with this, astrogliosis, as assessed by GFAP immunostaining, was markedly decreased in both $\Delta DD^{CreERT2}/5x\text{FAD}$ and $C259A^{CreERT2}/5x\text{FAD}$ mice at all time points of tamoxifen treatment (Fig. 4G,H). Interestingly, microglia, as assessed by Iba1 immunostaining, was only reduced in the mice that received tamoxifen at 2 months of age (Fig. 4I,J). To assess whether the effects observed at the tissue level had an impact on cognitive performance, we compared 5xFAD mice expressing p75^{NTR} variants at different times of the disease process in the Barnes maze. Strikingly, both $\Delta DD^{CreERT2}/5x\text{FAD}$ and $C259A^{CreERT2}/5x\text{FAD}$ mice showed improved learning ability compared with corn oil-injected controls during training, with no significant differences among the 2, 4, and 6 month injection groups (Fig. 5A,B). In the probe test, all three treatment groups spent significantly more time in the target quadrant, indicating improved spatial memory (Fig. 5C,D). Together, these results demonstrate that acute disruption of p75^{NTR} activity during advanced disease stages, i.e., after A β plaque formation and onset of cognitive impairment, is still able to confer beneficial effects to AD progression.

Discussion

Different forms of inactivation of the *Ngfr* gene, from null to point mutations to partial deletion, have been reported to show various degrees of neuroprotective effects in A β -based mouse models of AD when introduced constitutively during gestation (Knowles et al., 2009; Wang et al., 2011; Yi et al., 2021). As p75^{NTR} is expressed in several different cell types in the brain, e.g., neurons, glial cells, and endothelial cells, it has been unclear whether the beneficial effects afforded by its loss of function arise from all cell types or only one, and if so which one. Moreover, for therapeutic approaches targeting p75^{NTR} to be viable in AD patients, any form of interference with its activity needs to demonstrate beneficial effects during symptomatic stages of the disease, as this is the main cohort of patients that is normally recruited to clinical trials of AD. In this study, we have shown that replacement of native p75^{NTR} with signaling-impaired

variants of the receptor in forebrain excitatory neurons is sufficient to significantly alleviate neuropathological and behavioral outcomes in 5xFAD mice, one of the most aggressive mouse models of AD. Although the benefits attained in forebrain structures, namely, cerebral cortex and hippocampus, were comparable with those reached by a constitutive mutation from gestation, no reductions in A β plaque deposition were observed in the thalamus of either $\Delta DD^{Camk2a}/5x\text{FAD}$ or $C259A^{Camk2a}/5x\text{FAD}$ mice, indicating that the effects of these mutations on amyloid burden are brain region-autonomous. Significantly, however, spatial learning and memory (and to some degree also novelty recognition) were rescued to levels similar to those displayed by healthy, non-AD mice, in line with the importance of forebrain structures in these cognitive functions.

Our previous studies showed that signaling-deficient ΔDD and $C259A$ p75^{NTR} variants display significantly reduced internalization and increased partition to recycling endosomes in hippocampal neurons (Yi et al., 2021). One consequence of this is that other transmembrane proteins with an ability to interact and cointernalize with p75^{NTR}, such as APP, become similarly affected. Thus, both ΔDD and $C259A$ p75^{NTR} delay APP internalization thereby enhancing its availability to plasma membrane α -secretases at the expense of BACE1 β -secretase, which predominantly operates in acidic intracellular compartments (Das et al., 2013; Yi et al., 2021), leading to reduced A β production. In the present study, we found that selective expression of signaling-deficient ΔDD and $C259A$ p75^{NTR} variants in forebrain excitatory neurons significantly reduced the accumulation of the CTF β fragment, a product of APP cleavage by BACE1, while increasing sAPP α levels, which is generated by α -secretases, in the hippocampus of 5xFAD mice, indicating enhanced nonamyloidogenic APP processing. Thus, mechanistically, the reduction in A β levels observed after selective expression of ΔDD and $C259A$ p75^{NTR} variants in forebrain excitatory neurons of 5xFAD mice is likely the result of impaired APP intracellular trafficking, as demonstrated in our previous study (Yi et al., 2021).

With regard to the temporal aspects of interrupting normal p75^{NTR} function in AD, a striking result of our study is the significant amelioration of AD neuropathology and cognitive function achieved after acute disruption of p75^{NTR} activity during symptomatic AD stages, particularly at 6 months of age, a stage at which the 5xFAD model show pronounced levels of amyloid deposition, gliosis, and behavioral impairment. This finding is highly significant, as all current clinical trials for AD enroll patients that already show symptoms of cognitive impairment, and supports the development of therapeutic strategies targeting p75^{NTR} in AD. Encouragingly, a recent Phase II clinical trial in AD patients of a small molecule presented as a “modulator” of p75^{NTR} activity resulted in a measurable improvement in several

astroglia reflected by GFAP immunostaining in the hippocampus of different mouse strains as indicated. Histograms shows the percentage of hippocampal area occupied by GFAP immunostaining (mean \pm SD, $N = 6$ mice per group). Two-way ANOVA followed by Tukey's multiple-comparisons test. $**p < 0.01$, $****p < 0.0001$ versus Control/5xFAD. All mice included in this analysis were male. **D**, Quantification of microglia reflected by Iba1 immunostaining in the hippocampus of different mouse strains as indicated. Histograms shows the percentage of hippocampal area occupied by Iba1 immunostaining (mean \pm SD, $N = 6$ mice per group). Two-way ANOVA followed by Tukey's multiple-comparisons test. $***p < 0.001$, $****p < 0.0001$ versus Control/5xFAD. All mice included in this analysis were male. **E**, Immunostaining of GFAP and vimentin in the hippocampus of 9-month-old Control, Control/5xFAD, $\Delta DD^{Camk2a}/5x\text{FAD}$, and $C259A^{Camk2a}/5x\text{FAD}$ mice. Scale bar, 500 μm . **F**, Quantification of vimentin immunostaining in the hippocampus of different mouse strains as indicated. Histograms show the percentage of hippocampal area occupied by vimentin immunostaining (mean \pm SD, $N = 6$ mice per group). One-way ANOVA followed by Tukey's multiple-comparisons test. $***p < 0.001$, $****p < 0.0001$ versus Control/5xFAD. All mice included in this analysis were male. **G**, Immunostaining of reticulon 3 (RTN3) and A β plaques in the hippocampus of 9-month-old Control, Control/5xFAD, $\Delta DD^{Camk2a}/5x\text{FAD}$, and $C259A^{Camk2a}/5x\text{FAD}$ mice. Scale bar, 15 μm . **H**, Quantification of RTN3-positive dystrophic neurites in the hippocampus of different mouse strains as indicated. Histograms show the percentage of A β plaque area that overlapped with RTN3 immunostaining (mean \pm SD, $N = 6$ mice per group). One-way ANOVA followed by Tukey's multiple-comparisons test. $***p < 0.001$, $****p < 0.0001$ versus Control/5xFAD. All mice included in this analysis were male.

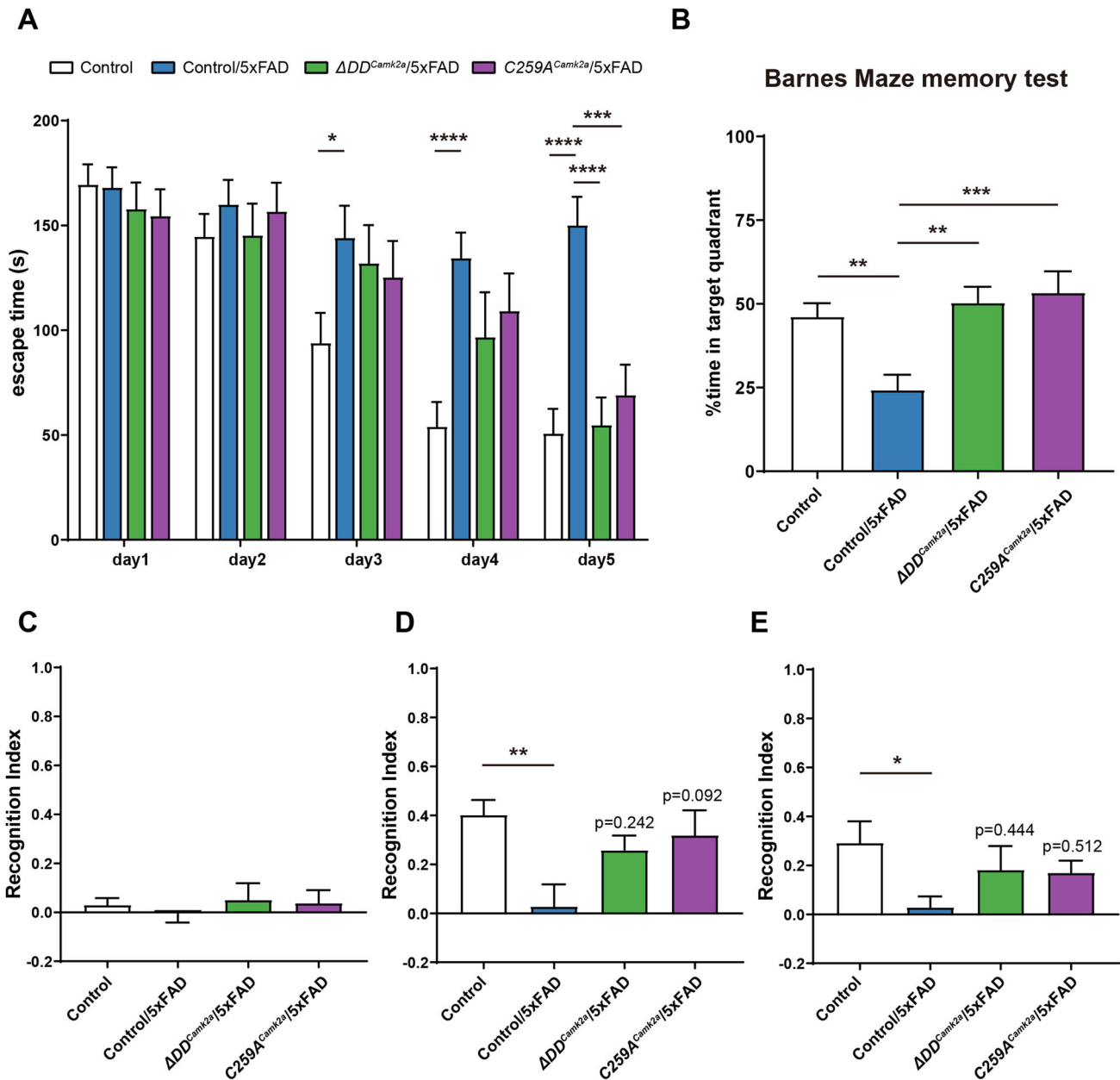


Figure 3. Improved learning and memory in 5xFAD mice expressing ΔDD and C259A p75^{NTR} variants in forebrain neurons. **A**, Training latency in the Barnes maze test of 6-month-old Control, Control/5xFAD, $\Delta DD^{Camk2a}/5xFAD$, and $C259A^{Camk2a}/5xFAD$ mice as indicated. Histograms show the escape time to find the tunnel in the training session of 5 consecutive days (mean \pm SEM). $N = 17$ (control and Control/5xFAD), 12 ($\Delta DD^{Camk2a}/5xFAD$), and 14 ($C259A^{Camk2a}/5xFAD$) mice per genotype, respectively. Two-way ANOVA followed by Tukey's multiple-comparisons test. * $p < 0.05$, ** $p < 0.01$, *** $p < 0.001$, **** $p < 0.0001$ versus Control/5xFAD. All mice included in this analysis were male. **B**, Percentage of time (mean \pm SEM) spent in the target quadrant of the Barnes maze test 3 h after training. One-way ANOVA followed by Tukey's multiple-comparisons test. * $p < 0.05$, ** $p < 0.01$ versus Control/5xFAD. **C–E**, Behavior performance in the novel object recognition (NOR) test of 6-month-old Control, Control/5xFAD, $\Delta DD^{Camk2a}/5xFAD$, and $C259A^{Camk2a}/5xFAD$ mice as indicated. Histograms show recognition index (mean \pm SEM) during training (**C**), 3 h after training (**D**, referred to as short-term memory), and 24 h after training (**E**, referred to as long-term memory). $N = 12$ (control), 15 (Control/5xFAD), 8 ($\Delta DD^{Camk2a}/5xFAD$), and 8 ($C259A^{Camk2a}/5xFAD$) mice per genotype, respectively. Two-way ANOVA followed by Tukey's multiple-comparisons test. * $p < 0.05$, ** $p < 0.01$ versus Control/5xFAD. All mice included in this analysis were male.

AD biomarkers as well as cognitive functions, although the latter did not reach statistical significance (Shanks et al., 2024). It is currently unknown how this drug affects p75^{NTR} signaling. In this regard, the results of our present study, particularly the effects of the C259A mutation in the transmembrane domain, provide a new direction for the development of molecules that tweak the activity of p75^{NTR} in a beneficial way, perhaps by targeting the transmembrane domain of the receptor, as shown in previous work from our laboratory (Goh et al., 2018; Lopes-Rodrigues and Ibáñez, 2025).

Unexpectedly, a comparable reduction in A β burden was observed in 9-month-old $\Delta DD^{CreERT2}/5xFAD$ and $C259A^{CreERT2}/5xFAD$ mice (roughly 50% of control 5xFAD) regardless of the time of TMX injection (whether 2, 4, or 6 months), suggesting that acute impairment of p75^{NTR} function in symptomatic AD does not reduce amyloid accumulation at a constant rate but up to a certain threshold level, roughly equivalent to that of 6-month-old control 5xFAD mice, covering $\sim 3\%$ of the hippocampus. Indeed, the level of amyloid accumulated at 9 months in the conditional mutants that received TMX at

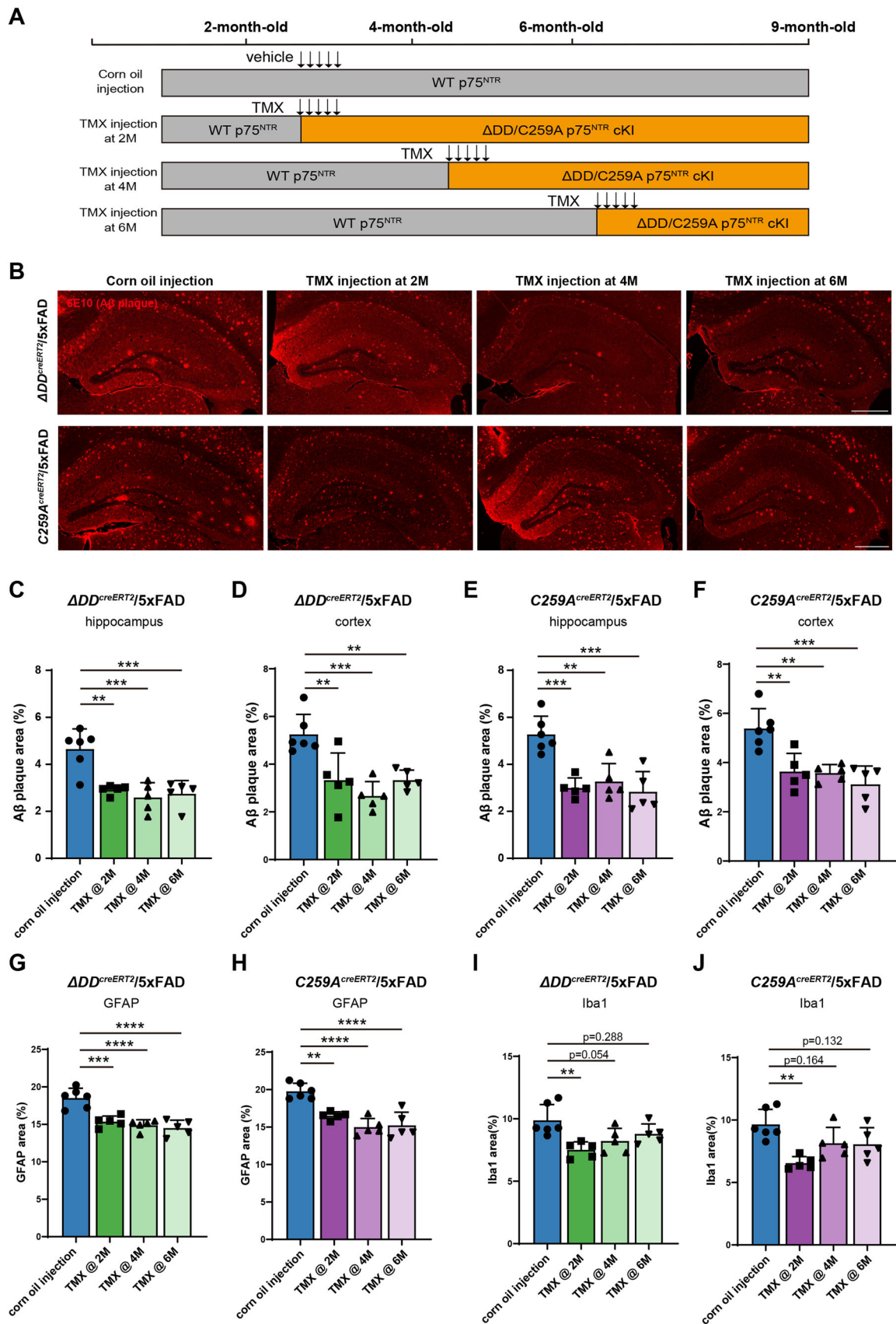


Figure 4. Significant amelioration of AD neuropathology after acute disruption of p75^{NTR} activity during symptomatic AD stages. **A**, Schematic illustration of tamoxifen administration paradigms. Tamoxifen was administered at 2, 4, or 6 months and analyses were conducted at 9 months of age. **B**, Immunostaining of Aβ plaques with 6E10 antibody in the hippocampus of $\Delta DD^{CreERT2}/5xFAD$ and $C259A^{CreERT2}/5xFAD$ 9-month-old mice treated with TMX at the indicated ages. Scale bar, 500 μm . **C**, **D**, Quantification of Aβ plaque burden in the hippocampus (**C**) and cortex (**D**) of $\Delta DD^{CreERT2}/5xFAD$ treated with corn oil or TMX as indicated. Histogram shows the percentage of hippocampal or cortical area occupied by Aβ plaques (mean \pm SD, $N = 5-6$ animals).

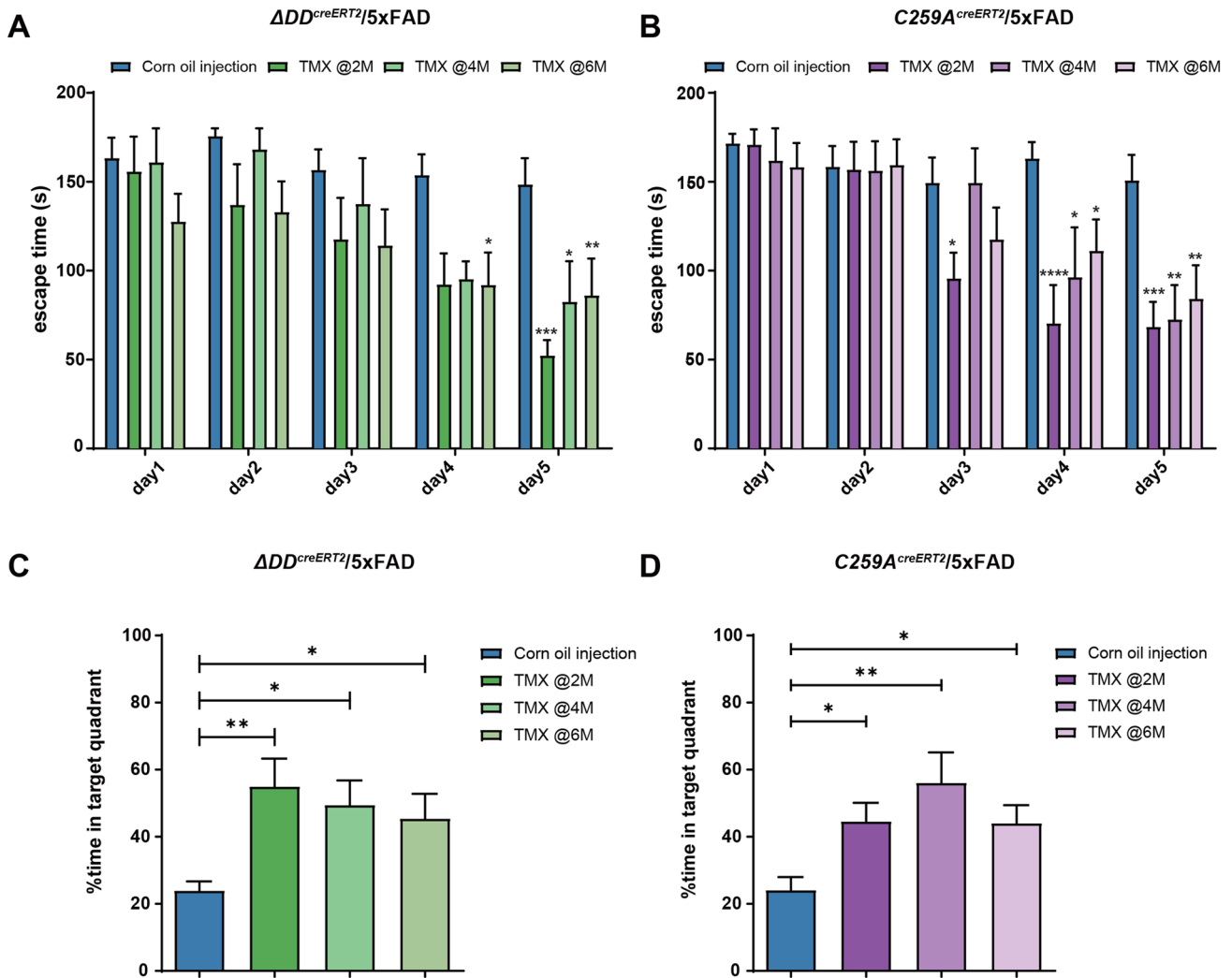


Figure 5. Significant improvement in cognitive function after acute disruption of p75^{NTR} activity during symptomatic AD stages. **A, B**, Training latency in the Barnes maze test of 9-month-old $\Delta DD^{CreERT2}/5xFAD$ (**A**) and $C259A^{CreERT2}/5xFAD$ (**B**) treated with corn oil or TMX as indicated. Histograms show the escape time to find the tunnel in the training session of 5 consecutive days (mean \pm SEM). In panel **A**, $N = 13$ (corn oil injection), 7 (TMX @2M), 7 (TMX @4M), and 12 (TMX @6M) mice per genotype, respectively. In panel **B**, $N = 15$ (corn oil injection), 10 (TMX @2M), 6 (TMX @4M), and 10 (TMX @6M) mice per genotype, respectively. Two-way ANOVA followed by Tukey's multiple-comparisons test. * $p < 0.05$, ** $p < 0.01$, *** $p < 0.001$, **** $p < 0.0001$ versus corn oil-injected mice. Both male and female mice are used. **C, D**, Percentage of time (mean \pm SEM) spent in the target quadrant 3 h after the last training of 9-month-old $\Delta DD^{CreERT2}/5xFAD$ (**C**) and $C259A^{CreERT2}/5xFAD$ (**D**) treated with corn oil or TMX as indicated. One-way ANOVA followed by Tukey's multiple-comparisons test. * $p < 0.05$, ** $p < 0.01$ versus corn oil-injected mice.

6 months was similar to the levels that control 5xFAD mice showed at 6 months, suggesting amyloid levels were stabilized at 6 months after TMX administration, staying constant for another 3 months. Intriguingly, despite comparable levels of amyloid burden, 6-month-old 5xFAD mice were cognitively impaired (Fig. 3) but 9 month conditional mutants that received TMX at 6 months were not (or much less so, Fig. 5), suggesting a

recovery of cognitive function that cannot solely be explained by A β plaque levels in the brain. Although microgliosis remained unchanged in conditional mutants that received TMX at 6 months, astrogliosis was reduced below the level of 6-month-old 5xFAD mice, but whether this was a contributing factor to their improved cognitive behavior is unclear at present. It is also possible that the mutations had beneficial effects on synapse

per group). All the mice assessed are males. One-way ANOVA followed by Tukey's multiple-comparisons test. ** $p < 0.01$, *** $p < 0.001$ versus corn oil-injected mice. **E, F**, Quantification of A β plaque burden in the hippocampus (**E**) and cortex (**F**) of $C259A^{CreERT2}/5xFAD$ treated with corn oil or TMX as indicated. Histogram shows the percentage of hippocampal or cortical area occupied by A β plaques (mean \pm SD, $N = 5-6$ animals per group). All the mice assessed are males. One-way ANOVA followed by Tukey's multiple-comparisons test. ** $p < 0.01$, *** $p < 0.001$ versus corn oil-injected mice. **G, H**, Quantification of astrogliosis reflected by GFAP immunostaining in the hippocampus of $\Delta DD^{CreERT2}/5xFAD$ (**G**) and $C259A^{CreERT2}/5xFAD$ (**H**) treated with corn oil or TMX as indicated. Histograms show the percentage of hippocampal area occupied by GFAP immunostaining (mean \pm SD, $N = 5-6$ mice per group). One-way ANOVA followed by Tukey's multiple-comparisons test. ** $p < 0.01$, *** $p < 0.0001$ versus corn oil-injected mice. All mice included in this analysis were male. **I, J**, Quantification of microgliosis reflected by Iba1 immunostaining in the hippocampus of $\Delta DD^{CreERT2}/5xFAD$ (**I**) and $C259A^{CreERT2}/5xFAD$ (**J**) treated with corn oil or TMX as indicated. Histograms show the percentage of hippocampal area occupied by Iba1 immunostaining (mean \pm SD, $N = 6$ mice per group). One-way ANOVA followed by Tukey's multiple-comparisons test. *** $p < 0.001$ versus corn oil-injected mice. All mice included in this analysis were male.

integrity or function beyond affecting APP processing or A β levels. Unlike A β plaque burden and astrogliosis, only the conditional mutants that received TMX at 2 months exhibited improved microgliosis when examined at 9 months, suggesting that microgliosis requires a longer time to resolve upon reduction of A β plaque accumulation.

In conclusion, our demonstration that neuron-specific impairment of p75^{NTR} function confers neuroprotection in a very aggressive model of AD—even at symptomatic stages—positions p75^{NTR} as a promising therapeutic target and opens new avenues for interventions that can be beneficial beyond early disease stages.

References

- Bach ME, Hawkins RD, Osman M, Kandel ER, Mayford M (1995) Impairment of spatial but not contextual memory in CaMKII mutant mice with a selective loss of hippocampal LTP in the range of the theta frequency. *Cell* 81:905–915.
- Barnes CA (1979) Memory deficits associated with senescence: a neurophysiological and behavioral study in the rat. *J Comp Physiol Psychol* 93:74–104.
- Beyreuther K, Masters CL (1991) Amyloid precursor protein (APP) and BZA4 amyloid in the etiology of Alzheimer's disease: precursor-product relationships in the derangement of neuronal function. *Brain Pathol* 1: 241–251.
- Bitan G, Kirkitadze MD, Lomakin A, Vollers SS, Benedek GB, Teplow DB (2003) Amyloid β -protein (A β) assembly: A β 40 and A β 42 oligomerize through distinct pathways. *Proc Natl Acad Sci U S A* 100:330–335.
- Bronfman FC, Fainzilber M (2004) Multi-tasking by the p75 neurotrophin receptor: sortilin things out? *EMBO Rep* 5:867–871.
- Chakravarthy B, Ménard M, Ito S, Gaudet C, Dal-Pra I, Armato U, Whitfield J (2012) Hippocampal membrane-associated p75NTR levels are increased in Alzheimer's disease. *J Alzheimers Dis* 30:675–684.
- Chao MV (2003) Neurotrophins and their receptors: a convergence point for many signalling pathways. *Nat Rev Neurosci* 4:299–309.
- Das U, Scott DA, Ganguly A, Koo EH, Tang Y, Roy S (2013) Activity-induced convergence of APP and BACE-1 in acidic microdomains via an endocytosis-dependent pathway. *Neuron* 79:447–460.
- Dechant G, Barde Y-A (2002) The neurotrophin receptor p75(NTR): novel functions and implications for diseases of the nervous system. *Nat Neurosci* 5:1131–1136.
- Deng Q, Wu C, Parker E, Liu TC-Y, Duan R, Yang L (2024) Microglia and astrocytes in Alzheimer's disease: significance and summary of recent advances. *Aging Dis* 15:1537–1564.
- Erdmann G, Schütz G, Berger S (2007) Inducible gene inactivation in neurons of the adult mouse forebrain. *BMC Neurosci* 8:63–63.
- Förner S, Kawachi S, Neumann J, Walker A, MacGregor GR, Green KN, LaFerla FM, Tenner AJ (2021) Development of new mouse strains containing alleles of loci associated with higher risk of late-onset Alzheimer's disease (LOAD). *Alzheimer's Dement* 17:e055651.
- Furukawa K, Sopher BL, Rydel RE, Begley JG, Pham DG, Martin GM, Fox M, Mattson MP (1996) Increased activity-regulating and neuroprotective efficacy of α -secretase-derived secreted amyloid precursor protein conferred by a C-terminal heparin-binding domain. *J Neurochem* 67:1882–1896.
- Goh ETH, Lin Z, Ahn BY, Lopes-Rodrigues V, Dang NH, Salim S, Berger B, Dymock B, Senger DL, Ibáñez CF (2018) A small molecule targeting the transmembrane domain of death receptor p75NTR induces melanoma cell death and reduces tumor growth. *Cell Chem Biol* 25:1485–1494.e5.
- Habib N, et al. (2020) Disease-associated astrocytes in Alzheimer's disease and aging. *Nat Neurosci* 23:701–706.
- Hardy J, Allsop D (1991) Amyloid deposition as the central event in the aetiology of Alzheimer's disease. *Trends Pharmacol Sci* 12:383–388.
- Hu X-Y, Zhang H-Y, Qin S, Xu H, Swaab DF, Zhou J-N (2002) Increased p75(NTR) expression in hippocampal neurons containing hyperphosphorylated tau in Alzheimer patients. *Exp Neurol* 178:104–111.
- Hu X-Y, Shi Q, Zhou X, He W, Yi H, Yin X, Gearing M, Levey A, Yan R (2007) Transgenic mice overexpressing reticulon 3 develop neuritic abnormalities. *EMBO J* 26:2755–2767.
- Ibáñez CF, Simi A (2012) P75 neurotrophin receptor signaling in nervous system injury and degeneration: paradox and opportunity. *Trends Neurosci* 35:431–440.
- Knowles JK, Rajadas J, Nguyen T-VV, Yang T, LeMieux MC, Griend LV, Ishikawa C, Massa SM, Wyss-Coray T, Longo FM (2009) The p75 neurotrophin receptor promotes amyloid-beta(1-42)-induced neuritic dystrophy in vitro and in vivo. *J Neurosci* 29:10627–10637.
- Lee H-G, Quintana FJ (2024) Astrocytes at the border of repair. *Nat Neurosci* 27:1445–1446.
- Liepinsh E, Ilag LL, Otting G, Ibáñez CF (1997) NMR structure of the death domain of the p75 neurotrophin receptor. *EMBO J* 16:4999–5005.
- Lopes-Rodrigues V, Ibáñez CF (2025) Impaired migration and lung invasion of human melanoma by a novel small molecule targeting the transmembrane domain of death receptor p75NTR. *EMBO Mol Med* 17:2661–2690.
- Madisen L, et al. (2010) A robust and high-throughput Cre reporting and characterization system for the whole mouse brain. *Nat Neurosci* 13: 133–140.
- Meziane H, Dodart J-C, Mathis C, Little S, Clemens J, Paul SM, Ungerer A (1998) Memory-enhancing effects of secreted forms of the β -amyloid precursor protein in normal and amnesic mice. *Proc Natl Acad Sci U S A* 95: 12683–12688.
- Mufson EJ, Kordower JH (1992) Cortical neurons express nerve growth factor receptors in advanced age and Alzheimer disease. *Proc Natl Acad Sci U S A* 89:569–573.
- Oakley H, et al. (2006) Intraneuronal beta-amyloid aggregates, neurodegeneration, and neuron loss in transgenic mice with five familial Alzheimer's disease mutations: potential factors in amyloid plaque formation. *J Neurosci* 26:10129–10140.
- Roux PP, Barker PA (2002) Neurotrophin signaling through the p75 neurotrophin receptor. *Prog Neurobiol* 67:203–233.
- Selkoe DJ (1991) The molecular pathology of Alzheimer's disease. *Neuron* 6: 487–498.
- Selkoe DJ (2000) Toward a comprehensive theory for Alzheimer's disease. Hypothesis: Alzheimer's disease is caused by the cerebral accumulation and cytotoxicity of amyloid β -protein. *Ann N Y Acad Sci* 924:17–25.
- Shanks HRC, Chen K, Reiman EM, Blennow K, Cummings JL, Massa SM, Longo FM, Börjesson-Hanson A, Windisch M, Schmitz TW (2024) P75 neurotrophin receptor modulation in mild to moderate Alzheimer disease: a randomized, placebo-controlled phase 2a trial. *Nat Med* 30:1761–1770.
- Singh D (2022) Astrocytic and microglial cells as the modulators of neuroinflammation in Alzheimer's disease. *J Neuroinflammation* 19:206.
- Stein TD, Anders NJ, DeCarli C, Chan SL, Mattson MP, Johnson JA (2004) Neutralization of transthyretin reverses the neuroprotective effects of secreted amyloid precursor protein (APP) in APPsw mice resulting in Tau phosphorylation and loss of hippocampal neurons: support for the amyloid hypothesis. *J Neurosci* 24:7707–7717.
- Strooper BD, Karran E (2016) The cellular phase of Alzheimer's disease. *Cell* 164:603–615.
- Tanaka K, Kelly CE, Goh KY, Lim KB, Ibáñez CF (2016) Death domain signaling by disulfide-linked dimers of the p75 neurotrophin receptor mediates neuronal death in the CNS. *J Neurosci* 36:5587–5595.
- Tsien JZ, Chen DF, Gerber D, Tom C, Mercer EH, Anderson DJ, Mayford M, Kandel ER, Tonegawa S (1996) Subregion- and cell type-restricted gene knockout in mouse brain. *Cell* 87:1317–1326.
- Underwood CK, Coulson EJ (2008) The p75 neurotrophin receptor. *Int J Biochem Cell Biol* 40:1664–1668.
- Vassar R, et al. (1999) β -Secretase cleavage of Alzheimer's amyloid precursor protein by the transmembrane aspartic protease BACE. *Science* 286:735–741.
- Vassar R, Kovacs DM, Yan R, Wong PC (2009) The beta-secretase enzyme BACE in health and Alzheimer's disease: regulation, cell biology, function, and therapeutic potential. *J Neurosci* 29:12787–12794.
- Vilar M, et al. (2009) Activation of the p75 neurotrophin receptor through conformational rearrangement of disulphide-linked receptor dimers. *Neuron* 62:72–83.
- Wang Y-J, et al. (2011) p75NTR regulates A β deposition by increasing A β production but inhibiting A β aggregation with its extracellular domain. *J Neurosci* 31:2292–2304.
- Yi C, Goh KY, Wong L, Ramanujan A, Tanaka K, Sajikumar S, Ibáñez CF (2021) Inactive variants of death receptor p75NTR reduce Alzheimer's neuropathology by interfering with APP internalization. *EMBO J* 40: e104450.